Environmental Science Nano

ROYAL SOCIETY OF CHEMISTRY

PAPER

View Article Online
View Journal | View Issue

Cite this: *Environ. Sci.: Nano*, 2020, 7, 2313

Realistic polyethylene terephthalate nanoplastics and the size- and surface coating-dependent toxicological impacts on zebrafish embryos†

Yunxia Ji,‡[a] Chuyu Wang, ‡[a] Yunqing Wang,*[ab] Longwen Fu,[a] Mingsan Man[a] and Lingxin Chen *[abc]

Nanoplastics (NPs) as pollutants in aquatic environments and as a public health issue due to their accumulation in food chains are of increasing concern. However, previous studies have employed mainly commercial, chemically synthesized polystyrene model particles. Commercial NPs made of polyethylene terephthalate (PET), which is widely used in drinking bottles and packaging, are rarely manufactured, and thus have not been frequently studied in the laboratory. This seriously limits our understanding of their real environmental and biological effects. Herein, we employ a simple method for producing PET NPs directly from plastic bottles, preserving the PET chemical properties, and mimicking the mechanical breakdown process of plastics in nature. Using developing zebrafish embryos as an animal model, we investigate the bioaccumulation and *in vivo* toxicity of the produced PET NPs, which have diameter sizes of 20, 60–80, and 800 nm and are capped by two dispersing agents, *i.e.*, BSA and SDS. This study demonstrates the size-dependent distribution and the size- and concentration-dependent toxicity of PET NPs in terms of hatching rate, heart rate, and ROS generation. It also reveals that the PET_{BSA} NP treatment groups exhibited higher-level abnormalities in heart rate and more severe oxidative damage than the PET_{SDS} NP treatment groups. Taken together, this work proposes a novel mechanical preparation protocol for PET NPs and provides evidence relating to the toxicity of environmentally relevant NPs towards aquatic organisms.

Received 4th May 2020,
Accepted 6th July 2020

DOI: 10.1039/d0en00464b

rsc.li/es-nano

Environmental significance

Nanoplastics (NPs) with a size of less than 100 nm have been discovered in both water ecosystems and wild aquatic organisms. Herein, we demonstrate a method to produce realistic NPs, taking polyethylene terephthalate (PET) NPs as an example. The PET NPs are prepared directly from plastic water bottles *via* a mechanical-breakdown process. The bioaccumulation and *in vivo* toxicity of the PET NPs on developing zebrafish embryos were investigated. The results demonstrate the size- and concentration-dependent toxicity of PET NPs from the aspects of embryo and larval hatching rates and heart rates, and the generation of reactive oxygen species. Taken together, this is the first proposed mechanical-preparation protocol for PET NPs, and this study provides evidence relating to the toxicity of realistic NPs towards aquatic organisms.

Introduction

Ever since the 1950s, plastic production has been increasing rapidly, reaching a total amount of 8300 million metric tonnes in 2015.[1] With only around 5% of plastic products recycled and 10% incinerated, the rest are released to landfill or into the natural environment. Lately, numerous studies have confirmed that plastic debris experiences a "weathering" effect such as organic matter coating the surface, photo-oxidation, and mechanical abrasion, breaking down into microplastics (MPs, <5 mm) and nanoplastics (NPs, 1–100 nm).[2,3] These particles have been found worldwide in the natural environment, including soil, seawater and sediments.[4–8] At so small a size, there is a potential risk that MP/NPs will be ingested (or penetrate) and be distributed within living organisms. How the particles interact with various biological systems and what their impacts really are have become of growing concern to environmental scientists, academia, and the public.

[a] *CAS Key Laboratory of Coastal Environmental Processes and Ecological Remediation, Shandong Key Laboratory of Coastal Environmental Processes, Yantai Institute of Coastal Zone Research, Chinese Academy of Sciences, Yantai 264003, China. E-mail: yqwang@yic.ac.cn, lxchen@yic.ac.cn; Fax: +86 535 2109130; Tel: +86 535 2109130*

[b] *Center for Ocean Mega-Science, Chinese Academy of Sciences, Qingdao 266071, China*

[c] *Laboratory for Marine Biology and Biotechnology, Pilot National Laboratory for Marine Science and Technology, Qingdao 266237, China*

† Electronic supplementary information (ESI) available. See DOI: 10.1039/d0en00464b

‡ These two authors contributed equally to this work.

Real MPs/NPs in aquatic environments emerge as larger plastics (*e.g.* bottles, plastic bags, nets) become subjected to physical abrasion, such as friction due to water movement, or scraping against stones, sand and rocks, or biological conditions such as digestive fragmentation within the gastric mill of Antarctic krill. The degraded MPs/NPs under natural conditions are thought to have the following characteristics: 1) they are heterologous in size and morphology. 2) They preserve the original chemical properties of polymers. 3) They interact with surrounding biological matter in the complex chemical environment. To date, a lot of work has been performed using daphnia, mussels, zebrafish, and algae as model species,[9–12] revealing that MPs/NPs are widespread in *in vivo* distribution and induce severe biological risks, such as developmental retardation, inflammatory response, neurotoxicity and even mortality.[13–17] Such studies, however, have employed mostly commercially manufactured MPs/NPs. These products were well defined in terms of size and surface chemistry, and usually had a spherical morphology, which differed substantially from their real-life counterparts from the aspects of many physical (morphology, surface roughness, density) and chemical (surface chemistry, polymerization degree, additive) properties. Research using commercially manufactured nanoplastics, whose physicochemical parameters (including size, shape, and charge) can be accurately manipulated, are necessary to provide basic information about nanoplastics' biological effect in determining the importance of these parameters. Yet, as our understanding of the nano-effect progresses, the environmental relevance of micro/nanoplastics used in laboratories must be improved to obtain results that correspond better to reality in *in vivo* behavior and toxicological studies.

To overcome the problem, some recent work has endeavored to propose new preparation protocols for MPs/NPs. For example, Magri *et al.* 2018 employed laser ablation of polymers to obtain PET nanoplastics. This method enabled researchers to produce nanoparticles with a controlled size distribution.[18] However, its disadvantages, including the limited amount obtained and the requirement for sophisticated equipment, increased the difficulty for wider application. More importantly, the PET NP products experienced a chemical change in composition, thus losing their chemical reality for biological assessment as model NPs. Rodríguez Hernández *et al.* 2019 produced PET NPs by precipitating PET dissolved in trifluoroacetic acid solution, nevertheless changing the physical nature of the material.[19] The studies mentioned above have made certain advances in the production of environmentally relevant MPs/NPs and provide helpful insights for new preparation protocols. However, they cannot totally represent real NPs in natural conditions in terms of morphology, surface roughness, and additives, among other things.

In this work, we propose a new method to prepare nanoplastics by the mechanical breakdown of plastic bottles with the aid of a kitchen blender and BSA and SDS as the dispersant. Compared with the PET particles reported above, the NPs in our study are more environmentally relevant. On the one hand, they are made of the plastic bottles used in everyday life, better representing the physicochemical properties of common plastic products. On the other hand, the mechanical breakdown protocol mimics one of the major degradation processes of plastics in nature. The PET NPs made could thus better represent the physiological interactions and biological effects of plastic particles under ecological conditions. Given that the intense mechanical breakdown process of NPs and their presence in different aquatic matrices lead to NPs being formed with different particle sizes and different capped surfactants, we predict the following consequences: 1) NPs will show differences in stability because of the different natural water conditions. 2) The different existing states and different surface chemistries will influence exposure scenarios and further interactions with aquatic organisms, and thus produce different biological effects. Using developing zebrafish embryos as an animal model, we further assess the uptake, distribution, and toxicity of the as-prepared PET NPs with different sizes and different capping agents in zebrafish embryos and larvae. This study explores a useful model for PET NP production and investigates the size- and capping agent-dependent toxicological effects of NPs.

Materials and methods

Chemicals and reagents

Polyethylene terephthalate (PET) pieces were cut from locally purchased mineral water bottles (Nongfu Spring). Nile red and sodium dodecyl sulfonate (SDS) were purchased from Sigma. Bovine serum albumin (BSA) was purchased from Beyotime Biotechnology. Tetrahydrofuran (THF) and dimethyl sulfoxide (DMSO) were purchased from Sinopharm Chemical Reagent Company. 2′,7′-Dichlorodihydrofluorescein diacetate (H2DCFDA) was purchased from MedChemExpress. Ultrapure water was used throughout this work.

Preparation of PET NP solutions

For nanoplastic preparation, 20 g of plastic sheet was broken into small pieces with a paper shredder. Two types of dispersants, BSA and SDS, were used to disperse the particles during mechanical breakdown. The plastic debris was removed into a beaker that contained 300 mL of 0.05% BSA solution or 0.01% SDS solution. To simplify the experiment, we used a hand blender (Panasonic MX-G51 600 W) to break down the plastics. Because such blenders were not designed to work at high speeds for a long time, which would generate excessive heat, we made simple modifications to the electrical circuits and subjected the blender to a working pattern of 1 min of blending alternating with 5 min of resting, for a total of 6 h.

After 6 h of blending, the supernatant was withdrawn with a syringe. Considering that the settling rate of nanoplastics is the key factor determining centrifugal speed,

the supernatant was subjected to differential centrifugation to obtain nanoparticles in different diameter ranges. The precipitate was collected after every centrifugation with the set speed, and a higher centrifugal speed was applied for further centrifugation of the suspension to obtain smaller particles. The speed of the rotor was set, respectively, at 500, 1000, 1500, 2000, 4000, 6000, 8000 and 10 000 rpm for 20 min each time. In order to reduce the overlap of various particle size ranges, precipitates centrifuged with 1000 (or 1500), 4000, and 10 000 rpm were used in the following studies. Each precipitate of a PET NP sample was suspended with BSA (0.05%) or SDS (0.1%) to maintain good dispersibility. Each PET nanoparticle solution was divided into two equal lots; one half was dried for 24 hours in a vacuum drying oven (Bo Xun, China) at 40 °C, followed by weighing with a millionth analytical balance (Sartorius, Germany), and the other half was diluted using 0.05% BSA or 0.1% SDS at a final concentration of 5 mg mL^{-1} which were stored at 4 °C until further use. SEM images of the NPs were captured on an S-4800 field emission scanning electron microscope (SEM, Hitachi, Japan), and SEM sizes were analyzed using Nano Measurer software. The dynamic light scattering (DLS) and zeta potential of the PET nanoparticle samples at a concentration of 1 ppm were measured on a Zetasizer NanoZS90 (Malvern Instruments, UK).

Labeling of PET NPs

The nanoparticle solutions (1 mg mL^{-1}, 1 mL) were mixed with 2 μL of Nile red (5×10^{-4} M, dissolved in THF), and were stirred for 2 h. The mixture solutions were then centrifuged at 14 000 rpm for 30 min, and were washed with 0.05% BSA solution or 0.01% SDS solution three times.

Zebrafish and exposure

Zebrafish were purchased from Shanghai FishBio Co. Ltd. All zebrafish experimental procedures were performed in accordance with the Guide for the Care and Use of Laboratory Animals (Ministry of Science and Technology of China, 2006) and were approved by the Animal Ethics Committee of Yantai Institute of Coastal Zone Research, Chinese Academy of Science. Zebrafish embryotoxicity test (ZFET) assays were performed according to previous methodology described in the report by Vogs *et al.* 2019.[20] Adult zebrafish (*Danio rerio*, AB wild-type) were maintained at 28 ± 0.5 °C in a 14 : 10 h light/dark cycle and were fed with brine shrimp twice daily. To obtain embryos, female and male zebrafish (3 : 2) were mixed at 5 PM and embryos were collected the next morning at 9 AM. Dead/unfertilized embryos were removed. The embryo exposure tests began from 6 hpf and continued until 144 hpf. Zebrafish embryos were placed in 4 mL of treated solution (n = 15 per treatment) in 12-well microplates which were then covered with lids.

Toxicity tests

In this study, PET nanoparticles in three particle sizes and with two different dispersants were tested. Each PET nanoparticle sample at a concentration of 5 mg mL^{-1} was diluted with 0.0001% BSA or SDS to the concentration required for exposure experiments. At 6 hpf, healthy embryos were exposed to PET NP treated solutions (n = 15, triplicate) or control groups. For treatment groups, 15 embryos each time were assigned to a pool containing 4 mL of the following solutions: PET solutions with 20 nm particle size and dispersed by BSA ($PET_{20\text{-}BSA}$) of 50 ppm, 10 ppm, and 1 ppm; $PET_{80\text{-}BSA}$ of 50 ppm, 10 ppm, and 1 ppm; $PET_{800\text{-}BSA}$ of 50 ppm, 10 ppm, and 1 ppm; $PET_{20\text{-}SDS}$ of 50 ppm, 10 ppm, and 1 ppm; $PET_{60\text{-}SDS}$ of 50 ppm, 10 ppm, and 1 ppm; and $PET_{800\text{-}SDS}$ of 50 ppm, 10 ppm, and 1 ppm. Control groups included 4 mL of 0.0001% BSA or SDS, and Milli-Q water. A total of 3 pools for each group were used for these assays (that is, 45 embryos/samples). The hatching rate was measured at 48 hpf, and survivorship and heart rate were measured daily from 48 to 96 hpf. Heart rate was assessed by counting beats for 15 s in 5 individuals for every treatment group. The use of anesthesia was avoided lest it influence heart rate.

Fluorescent distribution of PET NPs in zebrafish

At 6 h post-fertilization, healthy embryos were randomly assigned to 8 groups. 6 of them were NP treatment groups with 4 mL of Nile red-labelled PET NP (10 ppm) solutions with different sizes (20, 60–80, and 800 nm) and capping agents (BSA and SDS), and 2 control groups solely with Nile red (10 nM) in 0.0001% BSA or SDS solutions. There were 15 embryos in each group. The uptake and distribution of PET NPs was observed using a Leica SP8 confocal microscope (CLSM, Leica, Germany). 5 embryos or hatched larva were selected randomly at a time from each treatment group. The mean fluorescence intensity of the embryos and larvae was analyzed using Leica Application Suite X software equipped in a Leica SP8 confocal microscope.

ROS assays

For quantitative ROS generation, the exposure experiment was performed in 12-well cell culture plates; three wells were set up for each size (20, 60–80 and 800 nm) and each dispersant (BSA or SDS), with each well consisting of 15 embryos exposed for 120 h. Then, five larvae were randomly selected from each group. The larvae were washed with water three times and exposed to 10 μM of DCFH-DA fluorescent probe solution for 1 h. After anesthetizing the larvae with 0.016 M tricaine, the ROS production in the larvae was detected with a confocal microscope. The mean fluorescence intensity of the larvae was analyzed using Leica Application Suite X software equipped in a Leica SP8 confocal microscope.

Statistical analysis

Statistical analyses were performed with Graphpad Prism software (version 5.0, GraphPad Software Co., USA). Experimental data were statistically analyzed by the two-way analysis of variance followed by Bonferroni's multiple comparisons test. The normality of the data was checked (Shapiro–Wilk test) prior to analysis. Experimental data were expressed as means ± standard deviation (S.D.), and differences were considered statistically significant at $p < 0.05$.

Results and discussion

Preparation and characterization of PET NPs

In natural water bodies, there are numerous kinds of protein biosurfactants that have capping and stabilizing abilities towards NPs.[21] Similarly, surfactants are omnipresent in the environment, either naturally formed or released by human activities,[22] which can also act as effective NP dispersive reagents in liquid media. To mimic the mechanical breakdown process of plastic in the natural environment, two widely used NP dispersants, *i.e.*, BSA and SDS, respectively, from the two categories mentioned above, were selected for PET NP preparation considering their environmental meaning. As shown from the SEM images in Fig. 1A and B, PET NPs of different diameters ranging from ~20 nm, ~60–80 nm, to ~800 nm could be obtained by using different centrifugation speeds. In the mixtures, the zeta potentials of BSA-capped and SDS-capped PET NPs were between −20.0 and −25.5 mV, and −66.7 and −84.2 mV, respectively, which rendered NPs with good dispersity (Table S1†). Besides, the production yield of NPs prepared using the "top-down" method was quantitatively measured. The amount of NPs with different diameters ranging from ~20 nm to ~800 nm reached the few milligrams to a dozen milligrams level in a single batch from 20 g of initial PET sheets (Table S3†), which was sufficient for the toxicological assessments on zebrafish embryos.

The dispersants played an important role in the formation of PET NPs. During the breaking of raw PET with a blender, BSA and SDS were quickly adsorbed on the freshly formed hydrophobic PET surface, preventing the aggregation of small PET pieces and thus subjecting them to further rounds of breaking for the generation of smaller pieces. Different molecular binding modes are involved in the dispersant-PET NPs. For BSA, the binding mechanisms are non-specific attraction force,[23] the hydrophobic bonds induced by electric polarity changes of approaching molecules, van der Waals' force, and hydrogen bonds, among others.[24] PET NPs were well dispersed as they took advantage of the steric hindrance and negative repulsion provided by BSA coating. For SDS, its 12-carbon tail and a sodium sulfonate "head-group" gave it amphiphilic properties. When it was incorporated with PET NPs, the hydrophobic tails clustered around the surface of the particle, while the hydrophilic sodium sulfonate "head-group," which has a negative charge, pointed outwards to the water. When the PET solutions were prepared at a concentration of 0.1% for SDS, the levels of SDS created like-charge repulsion strong enough to stabilize the NPs.

Colloidal stability difference between BSA- and SDS-capped PET NPs

In the following, the as-prepared NPs samples were used for toxicological studies (Table S2†). Considering the low concentration of NPs and dispersants in real ecological conditions, the dilution effect on the dispersion of the NPs was investigated first. In addition, in order to reduce interference to the intrinsic toxicity effect of nanoplastics, we chose BSA and SDS with a concentration of 0.0001%, which exhibited good biocompatibility, to disperse the nanoplastics.[25–27] $PET_{20\text{-}BSA}$ and $PET_{20\text{-}SDS}$ with 0.05% BSA or 0.1% SDS were diluted to 0.0001% dispersant concentration, followed by DLS measurement at different time points. As shown in Fig. 1D, the initial DLS sizes of $PET_{20\text{-}BSA}$ and $PET_{20\text{-}SDS}$ were both around 180 nm (larger than the TEM size because of the surface corona). After the dispersant dilution, the DLS size of $PET_{20\text{-}BSA}$ remained unchanged, whereas that of $PET_{20\text{-}SDS}$ immediately expanded drastically to around 900 nm, and similar large sizes could be continuously detected within 24 h. This observation suggested that BSA-capped PET NPs were effectively dispersed when released into a larger water body, and the SDS-capped PET NPs formed an agglomeration shortly after the dilution of SDS. In addition, zeta potential changes in PET NPs after dilution were observed (Fig. S1†). The result showed that the zeta potentials of $PET_{20\text{-}BSA}$ increased slightly after the dispersant dilution (−25.5 ± 2.5 mV *versus* −22.8 ± 0.6 mV). By contrast, the zeta potentials of $PET_{20\text{-}SDS}$ increased significantly from −66.7 ± 6.8 mV to −23.2 ± 3.4 mV. The striking changes in surface charge of SDS-capped PET NPs before and after dilution may be one factor contributing to its colloidal instability.

As a macromolecule with a tertiary structure, BSA had strong affinity to PET NPs through multiple interaction modes and binding sites, such as van der Waals' force *via* the hydrophobic imidazole ring of histidine, the side chains of phenylalanine, and hydrogen bonds, or *via* hydrophilic chemical groups (–OH, ═O, –NH, ═NH).[24] Thus, despite the decreasing BSA concentration, a number of factors converged to create a stable dispersion of PET NPs. By contrast, the colloidal stability of linear SDS-capped NPs relied greatly on the concentration of SDS in the surroundings. When the PET solutions were prepared at a concentration of 0.1% for SDS (far larger than its CMC, 8×10^{-3} mol L^{-1}), a high density of SDS, resulting from the hydrophobic effect of the alkyl long chains, was adsorbed on the PET NP surface. The negatively charged terminal groups, pointing towards water, created enough negative charge and thus repulsion force between particles to achieve temporary colloidal stability. However, when the concentration of SDS was reduced to 0.0001%, the SDS–PET NP adsorption equilibrium was broken, resulting in the dissociation of SDS from PET NPs into water. The

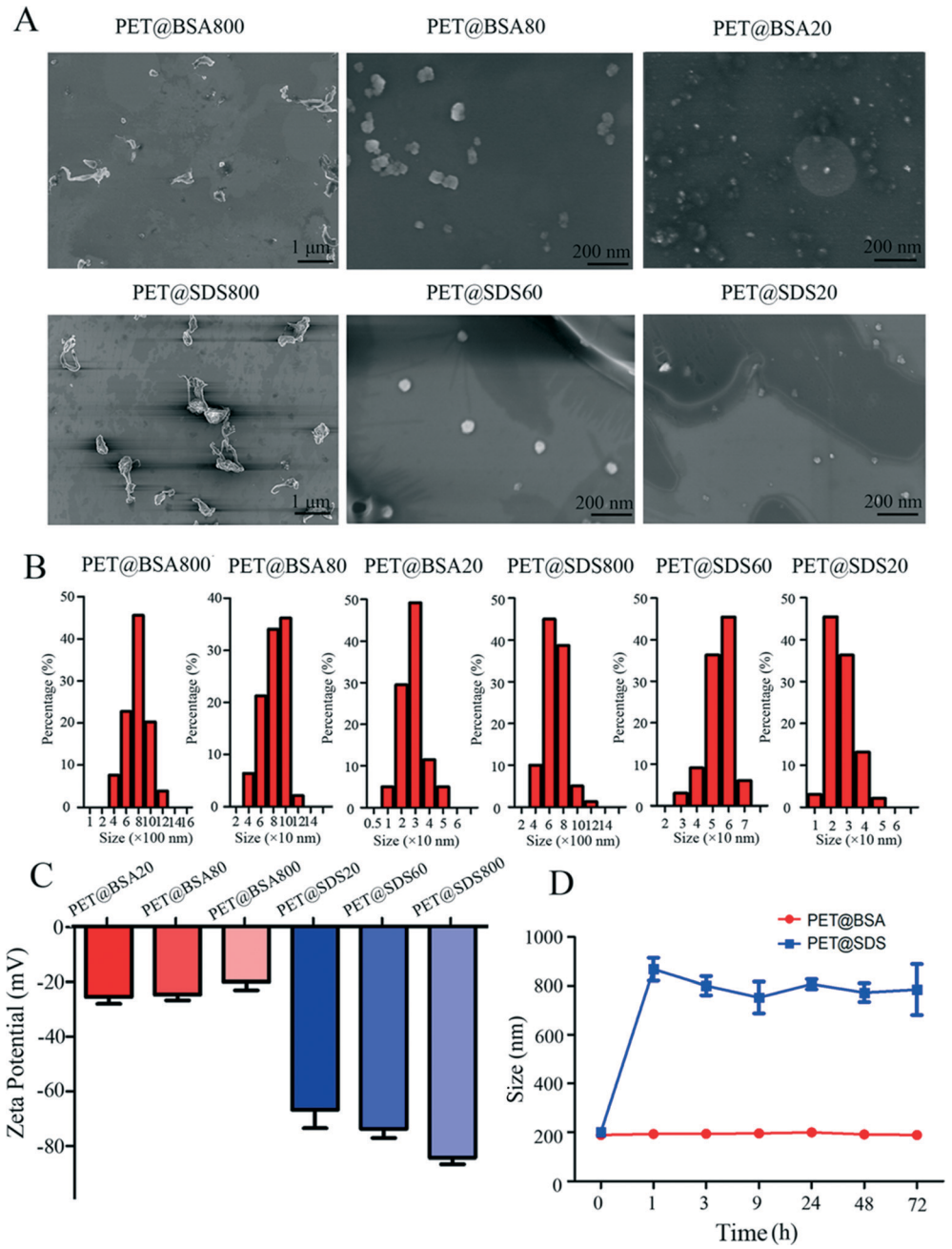

Fig. 1 (A) SEM images of differently sized PET NPs. (B) Particle sizes of PET NPs. (C) Zeta potentials of PET NPs. (D) DLS measurements of diluted $PET_{20\text{-}BSA}$ and $PET_{20\text{-}SDS}$ from 0 to 72 h.

remaining SDS on the PET NP surface failed to overcome the van der Waals' attractive force between NPs, leading to the formation of (sub)micro-sized PET particles.

Uptake of PET NPs in developing zebrafish

The uptake of PET NPs of different sizes was evaluated. As shown in Fig. 2 and S2–S4,† the fluorescence levels of $PET_{20\text{-}BSA}$ and $PET_{20\text{-}SDS}$ were consistently larger than those of $PET_{80\text{-}BSA}$ and $PET_{60\text{-}SDS}$, respectively, and those of nano-sized particles were consistently larger than those of $PET_{800\text{-}BSA}$ and $PET_{800\text{-}SDS}$, showing that most of the submicro-sized PET particles were blocked by the chorion and epidermis. Control groups (containing only free Nile red dye at the same concentration in NPs) showed very weak fluorescence which remained constant with increasing incubation time, suggesting that free dye (if there was any leakage from NPs or insoluble Nile red particles) would not interfere with the imaging results (Fig. 2B). All treatment groups showed more intense fluorescence than did the control groups (BSA, SDS). We also observed differences in the fluorescence levels between BSA and SDS treatment

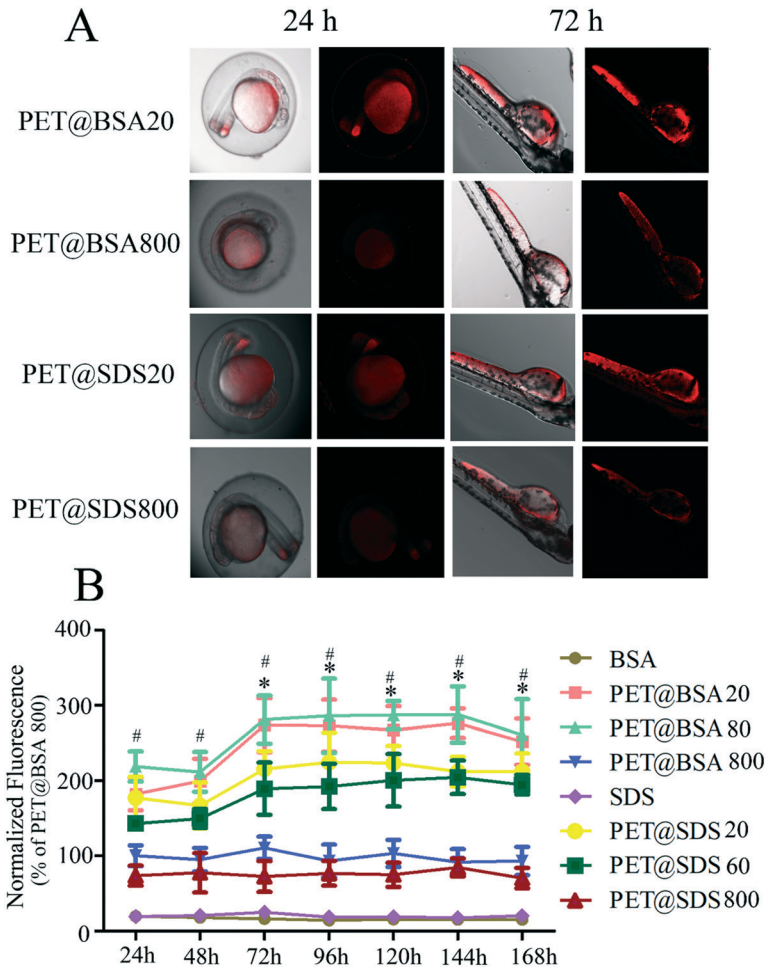

Fig. 2 The accumulation of PET NPs with different particle sizes (20, 800 nm) and with different capping agents (BSA, SDS) in zebrafish embryos and larvae (n = 5). (A) The fluorescent distribution of $PET_{20\text{-}BSA}$ and $PET_{800\text{-}BSA}$, and $PET_{20\text{-}SDS}$ and $PET_{800\text{-}SDS}$ at 24 and 72 hpf, measured with a Leica SP8 confocal microscope. (B) Normalized fluorescence levels of PET NPs, BSA, and SDS in zebrafish embryos and larvae from 24 to 168 hpf (n = 5). *$p < 0.05$, PET@BAS20 *versus* PET@SDS20. #$p < 0.05$, PET@BAS80 *versus* PET@SDS60.

groups. The fluorescence levels for $PET_{20\text{-}BSA}$ and $PET_{80\text{-}BSA}$ were consistently higher than those of $PET_{20\text{-}SDS}$ and $PET_{60\text{-}SDS}$, suggesting that the well-dispersed nanoparticles led to a higher bioaccumulation level in zebrafish embryos and larvae. In addition, the maintenance of clear fluorescence signals for $PET_{20\text{-}SDS}$ and $PET_{60\text{-}SDS}$ in agglomeration states indicated that, despite the aggregation of SDS-capped samples, some small-sized particles still passed through the chorion, which has pore canals with outer openings of 500 to 700 nm, as reported in previous studies.[28] Simultaneously, the agglomerated entities showed more distinguishable and stronger fluorescence, resulting in a high level of average fluorescence of SDS-dispersed PET detected with the confocal microscope.

The distribution of PET NPs in zebrafish embryos and larvae is shown in Fig. 3. At 24 hpf, apparent fluorescence could be observed not only on the chorion but also in the yolk, indicating that PET NPs could pass through the chorion. The clearer aggregations of $PET_{20\text{-}SDS}$ were visible on the surface of the chorions, which might be attributed to the low colloidal stability of SDS-capped NPs. From 48 hpf to 72 hpf, the fluorescence increased by up to 1 magnitude level in intensity, corresponding to the opening of the protruding mouth (oral pathway), the emergence of gills, and the inflation of the swim bladder.[29] In the same time period, fluorescence was also observed in the pericardium. From 72 hpf to 120 hpf, the larva resorbed the yolk sac, and the gastro-intestinal (GI) tract was functional. Fluorescence appeared in the GI tract, pancreas, liver, gall bladder, and pericardium. By 168 hpf, fluorescence was mostly observed in the GI tract and pancreas. However, fluorescence levels decreased in the pericardium, gall bladder and liver, which aligned with the excretion process of PET NPs.

Toxicity of PET NPs in developing zebrafish

Hatching, the emerging of young animals from their embryos, is fundamental for their survival and later development. Retardation of hatching could inhibit the uptake of nutrients, while failure to hatch means death. At

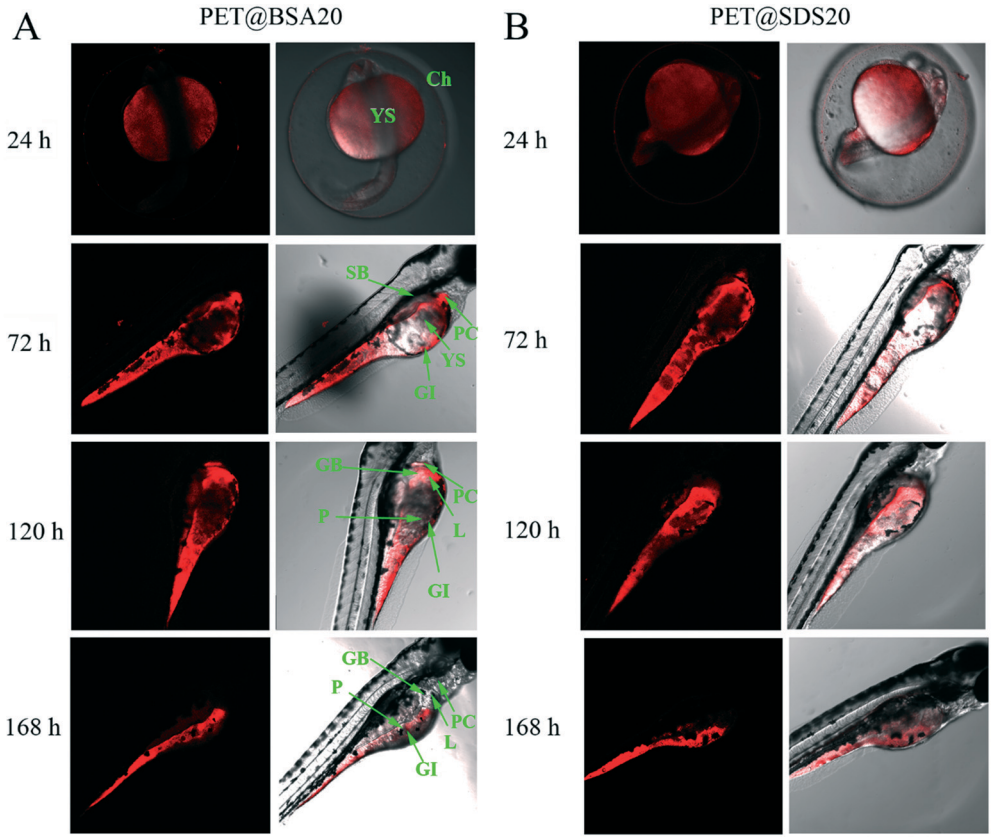

Fig. 3 Accumulation of fluorescent PET NPs with different capping agents (BSA and SDS) in zebrafish embryos and larvae at 24, 72, 120 and 168 hpf. Fluorescent distributions of $PET_{20\text{-}BSA}$ (A) and $PET_{20\text{-}SDS}$ (B). The letters in the images refer to various organs: (YS) yolk sac, (Ch) chorion, (YE) yolk extension, (PC) pericardium, (P) pancreas, (GB) gall bladder, (L) liver, (SB) swim bladder, and (GI) gastrointestinal tract.

48 hpf, we measured the hatching rate of zebrafish embryos exposed to PET NPs (Fig. 4). BSA-dispersed PET did show a generally larger hatching inhibition than did SDS-dispersed PET. In addition, BSA-capped nano-sized particles (20 nm and 80 nm) exhibited a hatching inhibition effect at higher tested concentrations (10 and 50 ppm), indicating that the hatching rate decreased in a size- and concentration-dependent manner. Meanwhile, 800 nm SDS capped NPs also showed side effects on the hatching of the eggs at 50 ppm, probably owing to the blocking of chorion pore canals.

Furthermore, the effect of PET NPs on the heart rate of zebrafish larvae was examined (Fig. 5). PET_{BSA} was found to induce a more dramatic influence than PET_{SDS} samples. At an early stage of 48 hpf, 20 nm and 80 nm BSA capped NPs significantly reduced the heart rate at higher tested concentrations (10 and 50 ppm), and 800 nm SDS capped NPs

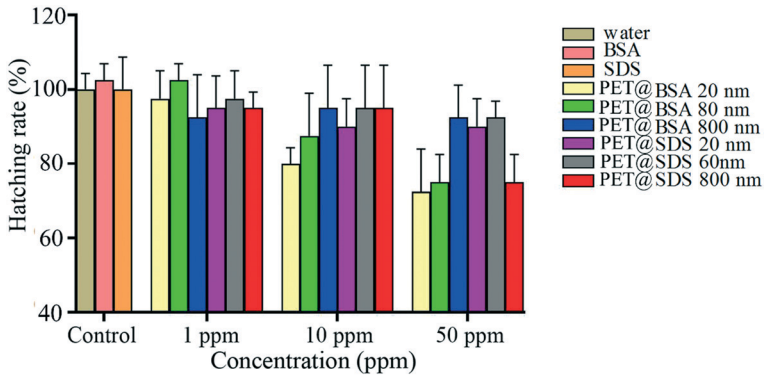

Fig. 4 Hatching rates (measured at 48 hpf) of zebrafish embryos exposed to PET NPs of different particle sizes (20, 60–80, and 800 nm), with different capping agents (BSA and SDS), and at different concentrations (1, 10, and 50 ppm).

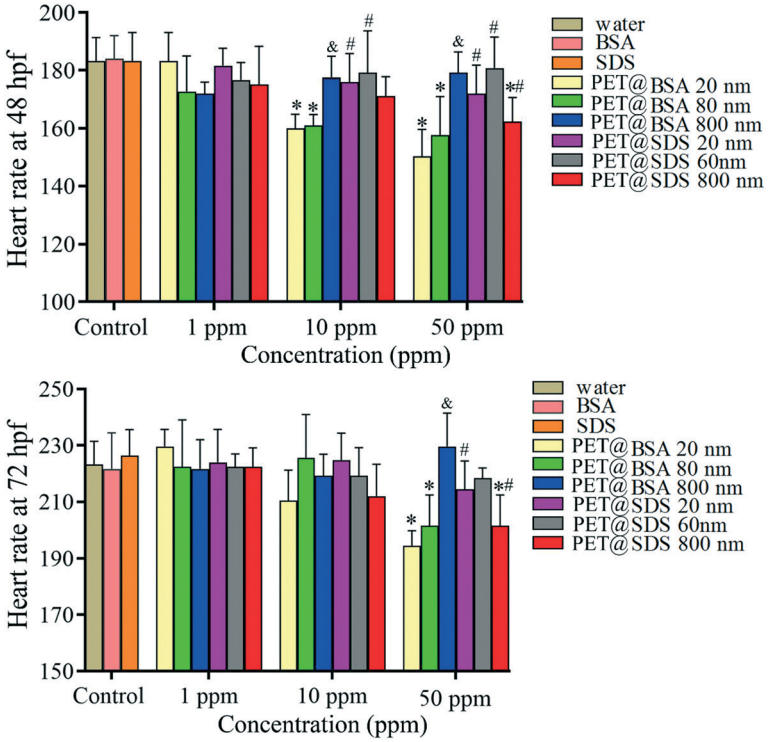

Fig. 5 Heart rates of zebrafish embryos and larvae exposed to PET NPs of different particle sizes (20, 60–80, and 800 nm), with different capping agents (BSA and SDS), and at different concentrations (1, 10, and 50 ppm). The asterisks refer to a significant heart rate decrease between the treatment groups and controls (n = 5). *$p < 0.05$, *versus* water group. &$p < 0.05$, *versus* smaller sized and same-capped PET NPs. #$p < 0.05$, *versus* same sized and different-capped PET NPs.

slightly reduced the heart rate at the highest NP concentration (50 ppm). In contrast, no disturbance was observed for SDS-capped nano-sized particles (20 nm and 60 nm) at the tested concentrations. In 72 hpf, the adverse effect was alleviated, suggesting that 20 nm and 80 nm BSA capped NPs showed a decreased heart rate only at the highest tested concentrations (50 ppm). Overall, BSA coating, small size and large concentration seemed to be the dominant factors in heart rate abnormality.

Consistent differences between BSA-capped and SDS-capped PET NPs in toxicity might be explained by two main factors. The first was the capping-agent-dependent NP size. PET_{BSA} NPs effectively dispersed in their original small size, allowing for free penetration through the embryo membrane. In contrast, PET_{SDS} NPs tended to aggregate and their sizes were distributed over a wide range. Only particles smaller than the pore size of the chorion could enter the embryos, and a large number of agglomerated NPs were observed to be blocked by the chorion (Fig. 2A). Previous studies have reported that the accumulation of nanoparticles on the chorion blocks the pores that transport oxygen/carbon dioxide and nutrients, thus delaying or inhibiting embryonic development.[30–32] This should be a key factor for the hatching disturbance effect of PET_{SDS} NPs. The uncontrollable particle size of PET_{SDS} NPs resulted in deviations in hatching rate results, which was also a sign of the toxic mechanism of blocking by NPs.

The second possible factor was the effect of NPs on intrinsic molecules in zebrafish embryos. Some previous studies have shown that the initial protein corona would continue to interact with other proteins in biological systems through non-specific protein–protein attraction, producing a remarkable coalescence effect on NPs,[1,33–35] while other studies observed the dispersion effect of organic matter on NPs, consistent with our results.[36–38] Either way, the adsorption of intrinsic key proteins and enzymes upon NPs could induce conformational structural changes. For instance, Brandes *et al.* in 2006 reported that adsorption of protein onto ceramic particles induced destabilization and loss of alpha-helical structure.[39] Lundqvist *et al.* in 2019 observed that the particle curvature of silica nanoparticles strongly influenced the amount of conformational changes in human carbonic anhydrase upon adsorption.[40] This effect would deliver further adverse biological activities of the nanoparticles, including longer retention time *in vivo*,[36] anti-inflammatory response,[41] and DNA damage.[24] Upon penetration into the embryo, the NPs would interact with the intrinsic functional biomolecules. In many fish species, the hatching gland cells are responsible for releasing chlorinase that kickstarts the initiation of hatching gene-expression, enabling the breakdown of eggs by the newborn fish.[42] Thus, the inhibition (blocking) of the secretory functions of the hatching gland cell, or malfunction of chlorinase induced by NP adsorption, could be reasons behind the reduction in hatching rate. Similarly, the formation and bio-interaction of protein corona could also explain the more severe heart rate disturbance shown in PET_{BSA} NP treatment groups.

What is more, the results indicated a size- and dose-dependent toxic effect. In treatment groups using the same dispersant, smaller particle size and higher concentration seemed to be the dominant factors contributing to PET NP toxicity. A smaller NP size was more inclined to penetrate and accumulate in the embryo, resulting in greater toxicity impacts. Most of the toxic effects were not observed for all PET NPs with a concentration of 1 ppm.

ROS detection

Due to the large specific surface area, high reactivity and electron density, plastic particles exposed to the acidic environment of lysosomes or mitochondria can induce the generation of reactive oxygen species.[43,44] Changes in ROS content reflect the level of lipid peroxidation and cellular damage in the body. In this study, the embryos were incubated in a culture medium containing PET NPs of different sizes and with different capping agents for 120 hpf. It was observed that the ROS content increased significantly and accumulated mainly in the heart and spine (Fig. 6), suggesting that cellular damage was inflicted by PET NPs on zebrafish embryonic development. ROS content was shown to be dependent on the type of capping agent and the particle size. Generally, BSA-capped particles induced more ROS content than did SDS-dispersed PET particles. Nano-sized

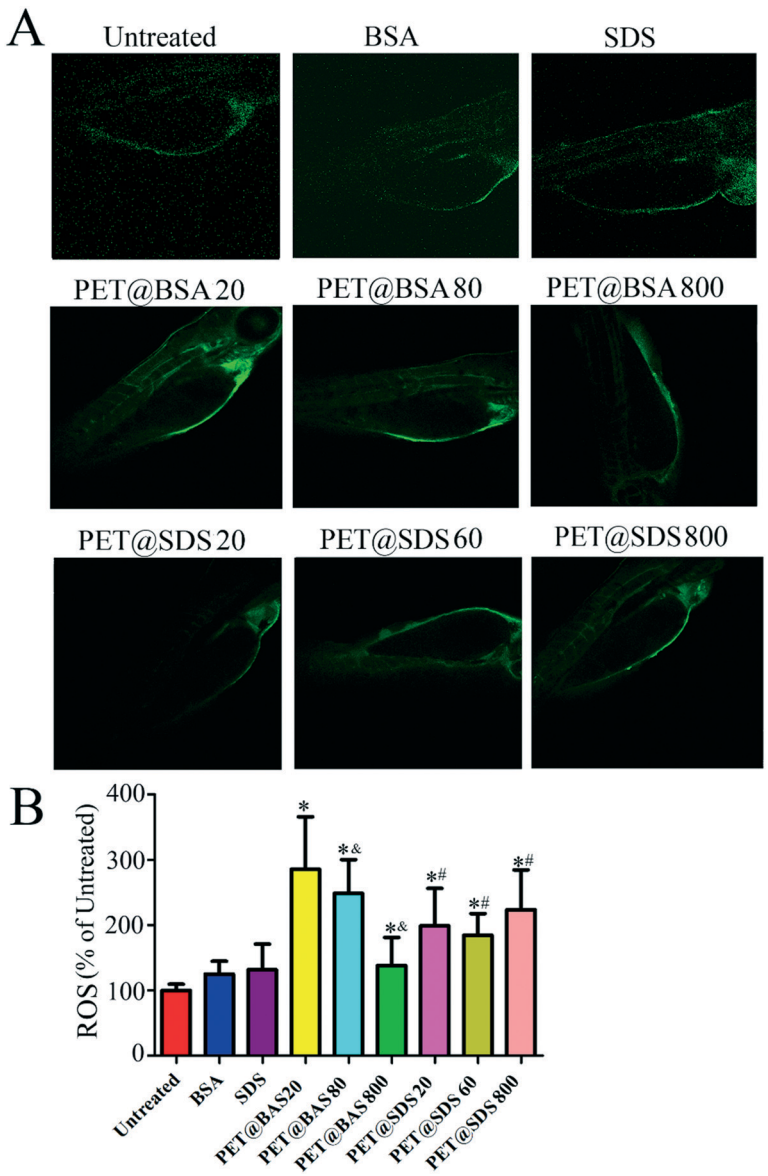

Fig. 6 Oxidative damage in zebrafish larvae. (A) Fluorescent images of ROS generation in zebrafish larvae at 120 hpf exposed to PET NPs with different particle sizes (20, 60–80, and 800 nm) and different capping agents (BSA and SDS) at a concentration of 10 ppm. (B) The quantitative analysis of ROS production in treatment groups and controls. *$p < 0.05$, *versus* water group. &$p < 0.05$, *versus* smaller-sized and same-capped PET NPs. #$p < 0.05$, *versus* same-sized and different-capped PET NPs.

particles induced more ROS content than did submicro-sized particles in PET_{BSA} NP treatment groups, which was possibly due to the larger amount of embryo uptake and thus more severe cell membrane and mitochondrial damage. By contrast, the ROS level in zebrafish larvae exposed to 800 nm SDS capped NPs was higher compared to those exposed to 20 nm or 60 nm SDS capped nano-sized particles. This might be accounted for by the aggregations of larger PET_{SDS} NPs, which were more capable of blocking the chorion pores. This result revealed that PET NPs were able to trigger ROS generation in a size- and dispersing agent-dependent manner, one of the underlying factors for the observed disturbance in hatching and heart rate.

Conclusions

In this study, we provide a simple method that mimics the natural breakdown process *via* mechanical force to produce environmentally relevant PET nanoparticles in large amounts and with the chemical properties of PET preserved. We evaluated the distribution of and cellular damage induced by three differently sized PET NPs capped with two dispersing agents in developing zebrafish embryos. Size-dependent and dispersing-agent-dependent uptake and accumulation of PET NPs, abnormalities in hatching rate and heart rate, and the generation of oxidative stress were observed. What is more, our results highlight the importance of the eco-corona on the colloidal stability and biological toxicity of NPs.

Conflicts of interest

There are no conflicts to declare.

Acknowledgements

Financial support from the National Natural Science Foundation of China (81573393, 21976209), the Science and Technology Development Plan of Shandong Province of China (2019GSF108047), the Youth Innovation Promotion Association CAS (2017256), the Instrument Developing Project of the Chinese Academy of Sciences (YZ201662), the Technical Innovation Project of Instrument Function Development of the Chinese Academy of Sciences, and the Taishan Scholar Project Special Funding (No. ts20190962), is gratefully acknowledged.

References

1 R. Geyer, J. R. Jambeck and K. L. Law, Production, use, and fate of all plastics ever made, *Sci. Adv.*, 2017, **3**, 1–5.
2 R. C. Thompson, Y. Olsen, R. P. Mitchell, A. Davis, S. J. Rowland, A. W. G. John, D. McGonigle and A. E. Russell, Lost at sea: where is all the plastic?, *Science*, 2004, **304**, 838.
3 A. A. Koelmans, E. Besseling and W. J. Shim, Nanoplastics in the aquatic environment, in *Critical Review. Marine Anthropogenic Litter*, Springer International Publishing, 2015, pp. 325–340.
4 Z. Dai, H. Zhang, Q. Zhou, Y. Tian, T. Chen, C. Tu, C. Fu and Y. Luo, Occurrence of microplastics in the water column and sediment in an inland sea affected by intensive anthropogenic activities, *Environ. Pollut.*, 2018, **242**, 1557–1565.
5 J. P. Da Costa, Micro- and nanoplastics in the environment: research and policymaking, *Curr. Opin. Environ. Sci. Health.*, 2018, **1**, 12–16.
6 O. S. Alimi, J. F. Budarz, L. M. Hernandez and N. Tufenkji, Microplastics and nanoplastics in aquatic environments: aggregation, deposition, and enhanced contaminant transport, *Environ. Sci. Technol.*, 2018, **52**, 1704–1724.
7 N. A. Welden and A. L. Lusher, Impacts of changing ocean circulation on the distribution of marine microplastic litter, *Integr. Environ. Assess. Manage.*, 2017, **13**, 483–487.
8 A. O. Debrot, H. W. Meesters, P. S. Bron and R. de Leon, Marine debris in mangroves and on the seabed: largely-neglected litter problems, *Mar. Pollut. Bull.*, 2013, **72**, 1.
9 S. Rist, A. Baun and N. B. Hartmann, Ingestion of micro- and nanoplastics in daphnia magna – quantification of body burdens and assessment of feeding rates and reproduction, *Environ. Pollut.*, 2017, **228**, 398–407.
10 S. Rist, A. Baun, R. Almeda and N. B. Hartmann, Ingestion and effects of micro- and nanoplastics in blue mussel (mytilus edulis) larvae, *Mar. Pollut. Bull.*, 2019, **140**, 423–430.
11 L. Lei, S. Wu, S. Lu, M. Liu, Y. Song, Z. Fu, H. Shi, K. M. Raley-Susman and D. He, Microplastic particles cause intestinal damage and other aadverse effects in zebrafish danio rerio and nematode caenorhabditis elegans, *Sci. Total Environ.*, 2018, **619**, 1–8.
12 Q. Chen, M. Gundlach, S. Yang, J. Jiang, M. Velki, D. Yin and H. Hollert, Quantitative investigation of the mechanisms of microplastics and nanoplastics toward zebrafish larvae locomotor activity, *Sci. Total Environ.*, 2017, **584**, 1022–1031.
13 M. Van Pomeren, N. R. Brun, W. Peijnenburg and M. G. Vijver, Exploring uptake and biodistribution of polystyrene (nano)particles in zebrafish embryos at different developmental stages, *Aquat. Toxicol.*, 2017, **190**, 40–45.
14 L. C. De Sa, M. Oliveira, F. Ribeiro, T. L. Rocha and M. N. Futter, Studies of the effects of microplastics on aquatic organisms: what do we know and where should we focus our efforts in the future?, *Sci. Total Environ.*, 2018, **645**, 1029–1039.
15 C.-B. Jeong, H.-M. Kang, M.-C. Lee, D.-H. Kim, J. Han, D.-S. Hwang, S. Souissi, S.-J. Lee, K.-H. Shin, H. G. Park and J.-S. Lee, Adverse effects of microplastics and oxidative stress-induced MAPK/Nrf2 pathway-mediated defense mechanisms in the marine copepod paracyclopina nana, *Sci. Rep.*, 2017, **7**, 1–11.
16 J. A. Pitt, J. S. Kozal, N. Jayasundara, A. Massarsky, R. Trevisan, N. Geitner, M. Wiesner, E. D. Levin and R. T. Di Giulio, Uptake, tissue distribution, and toxicity of polystyrene nanoparticles in developing zebrafish (Danio rerio), *Aquat. Toxicol.*, 2018, **194**, 185–194.
17 L. M. Skjolding, G. Asmonaite, R. I. Jolck, T. L. Andresen, H. Selck, A. Baun and J. Sturve, An assessment of the importance

of exposure routes to the uptake and internal localisation of fluorescent nanoparticles in zebrafish (Danio rerio), using light sheet microscopy, *Nanotoxicology*, 2017, **11**, 351–359.

18 D. Magri, P. Sanchez-Moreno, G. Caputo, F. Gatto, M. Veronesi, G. Bardi, T. Catelani, D. Guarnieri, A. Athanassiou, P. P. Pompa and D. Fragouli, Laser ablation as a versatile tool to mimic polyethylene terephthalate nanoplastic pollutants: characterization and toxicology assessment, *ACS Nano*, 2018, **12**, 7690–7700.

19 A. G. Rodríguez Hernández, J. A. Muñoz Tabares, J. C. Aguilar Guzmán and R. Vazquez Duhalt, A novel and simple method for polyethylene terephthalate (PET) nanoparticle production, *Environ. Sci.: Nano*, 2019, **6**, 2031–2036.

20 C. Vogs, G. Johanson, M. Näslund, S. Wulff, M. Sjödin, M. Hellstrandh, J. Lindberg and E. Wincent, Toxicokinetics of perfluorinated alkyl acids influences their toxic potency in the zebrafish embryo (Danio rerio), *Environ. Sci. Technol.*, 2019, **53**, 3898–3907.

21 A. Cooper and M. W. Kennedy, Biofoams and natural protein surfactants, *Biophys. Chem.*, 2010, **151**, 96–104.

22 T. Ivankovic and J. Hrenovic, Surfactants in the environment, *Arh. Hig. Rada Toksikol.*, 2010, **61**, 95–110.

23 M. S. Ehrenberg, A. E. Friedman, J. N. Finkelstein, G. Oberdorster and J. L. McGrath, The influence of protein adsorption on nanoparticle association with cultured endothelial cells, *Biomaterials*, 2009, **30**, 603–610.

24 P. M. Gopinath, V. Saranya, S. Vijayakumar, M. Mythili Meera, S. Ruprekha, R. Kunal, A. Pranay, J. Thomas, A. Mukherjee and N. Chandrasekaran, Assessment on interactive prospectives of nanoplastics with plasma proteins and the toxicological impacts of virgin, coronated and environmentally released-nanoplastics, *Sci. Rep.*, 2019, **9**(8860), 1–15.

25 J.-Y. Xue, X. Li, M.-Z. Sun, Y.-P. Wang, M. Wu, C.-Y. Zhang, Y.-N. Wang, B. Liu, Y.-S. Zhang, X. Zhao and X.-Z. Feng, An assessment of the impact of SiO2 nanoparticles of different sizes on the rest/wake behavior and the developmental profile of zebrafish larvae, *Small*, 2013, **9**, 3161–3168.

26 U. Taylor, D. Tiedemann, C. Rehbock, W. A. Kues, S. Barcikowski and D. Rath, Influence of gold, silver and gold-silver alloy nanoparticles on germ cell function and embryo development, *Beilstein J. Nanotechnol.*, 2015, **6**, 651–664.

27 P. Paramita, S. N. Sethu, N. Subhapradha, V. Ragavan, R. Ilangovan, A. Balakrishnan, N. Srinivasan, R. Murugesan and A. Moorthi, Neuro-protective effects of nano-formulated hesperetin in a traumatic brain injury model of Danio rerio, *Drug Chem. Toxicol.*, 2020, 1–8.

28 Diplom-Biologist Kirsten Henn, For the degree of Doctor of Natural Sciences, Limits of the fish embryo toxicity test with *Danio rerio* as an alternative to the acute fish toxicity test. Dissertation Submitted to the Combined Faculties for the Natural Sciences and for Mathematics of the Ruperto-Carola, *PhD thesis*, University of Heidelberg, Germany, 2011.

29 C. B. Kimmel, W. W. Ballard, S. R. Kimmel, B. Ullmann and T. F. Schilling, Stages of embryonic-development of the zebrafish, *Dev. Dyn.*, 1995, **203**, 253–310.

30 X. Zhao, S. Wang, Y. Wu, H. You and L. Lv, Acute ZnO nanoparticles exposure induces developmental toxicity, oxidative stress and DNA damage in embryo-larval zebrafish, *Aquat. Toxicol.*, 2013, **136**, 49–59.

31 W. Bai, Z. Zhang, W. Tian, X. He, Y. Ma, Y. Zhao and Z. Chai, Toxicity of Zinc oxide nanoparticles to zebrafish embryo: A physicochemical study of toxicity mechanism, *J. Nanopart. Res.*, 2009, **12**, 1645–1654.

32 J. Duan, Y. Yu, H. Shi, L. Tian, C. Guo, P. Huang, X. Zhou, S. Peng and Z. Sun, Toxic effects of silica nanoparticles on zebrafish embryos and larvae, *PLoS One*, 2013, **8**, e74606.

33 A. C. Greven, T. Merk, F. Karagoz, K. Mohr, M. Klapper, B. Jovanovic and D. Palic, Polycarbonate and polystyrene nanoplastic particles act as stressors to the innate immune system of fathead minnow (pimephales promelas), *Environ. Toxicol. Chem.*, 2016, **35**, 3093–3100.

34 K. Mohr, Aggregation behavior of polystyrene-nanoparticles in human blood serum and its impact on the *in vivo* distribution in mice, *J. Nanomed. Nanotechnol.*, 2014, **05**, 194–207.

35 F. Barbero, L. Russo, M. Vitali, J. Piella, I. Salvo, M. L. Borrajo, M. Busquets-Fite, R. Grandori, N. G. Bastus, E. Casals and V. Puntes, Formation of the protein corona: the interface between nanoparticles and the immune system, *Semin. Immunol.*, 2017, **34**, 52–60.

36 X. Wang, D. Liang, Y. Wang, Q. Ma, B. Xing and W. Fan, Effects of organic matter on uptake and intracellular trafficking of nanoparticles in trahymena thermophila, *Environ. Sci.: Nano*, 2019, **6**, 2116–2128.

37 F. Catalano, L. Accomasso, G. Alberto, C. Gallina, S. Raimondo, S. Geuna, C. Giachino and G. Martra, Factors ruling the uptake of silica nanoparticles by mesenchymal stem cells: agglomeration *versus* dispersions, absence *versus* presence of serum proteins, *Small*, 2015, **11**, 2919–2928.

38 J. Gao, K. Powers, Y. Wang, H. Zhou, S. M. Roberts, B. M. Moudgil, B. Koopman and D. S. Barber, Influence of suwannee river humic acid on particle properties and toxicity of silver nanoparticles, *Chemosphere*, 2012, **89**, 96–101.

39 N. Brandes, P. B. Welzel, C. Werner and L. W. Kroh, Adsorption-induced conformational changes of proteins onto ceramic particles: differential scanning calorimetry and FTIR analysis, *J. Colloid Interface Sci.*, 2006, **299**, 56–69.

40 M. Lundqvist, I. Sethson and B. H. Jonsson, Protein adsorption onto silica nanoparticles: conformational changes depend on the particles' curvature and the protein stability, *Langmuir*, 2004, **20**, 10639–10647.

41 D. Dutta, S. K. Sundaram, J. G. Teeguarden, B. J. Riley, L. S. Fifield, J. M. Jacobs, S. R. Addleman, G. A. Kaysen, B. M. Moudgil and T. J. Weber, Adsorbed proteins influence the biological activity and molecular targeting of nanomaterials, *Toxicol. Sci.*, 2007, **100**, 303–315.

42 F. I. Aksakal and A. Ciltas, Impact of copper oxide nanoparticles (CuO NPs) exposure on embryo development and expression of genes related to the innate immune system of zebrafish (Danio rerio), *Comp. Biochem. Physiol., Part C: Toxicol. Pharmacol.*, 2019, **223**, 78–87.

43 M. G. Bexiga, J. A. Varela, F. Wang, F. Fenaroli, A. Salvati, I. Lynch, J. C. Simpson and K. A. Dawson, Cationic nanoparticles induce Caspase 3-, 7- and 9-mediated cytotoxicity in a human astrocytoma cell line, *Nanotoxicology*, 2011, **5**, 557–567.

44 L. Li, S. Sun, L. Tan, Y. Wang, L. Wang, Z. Zhang and L. Zhang, Polystyrene nanoparticles reduced ROS and inhibited ferroptosis by triggering lysosome stress and TFEB nucleus translocation in a size-dependent manner, *Nano Lett.*, 2019, **19**, 7781–7792.